

Optimization of Multilayer Microwave Absorbers using Multi-strategy Improved Gold Rush Optimizer

Yi Ming Zong¹, Wei Bin Kong¹, Jia Pan Li², Lei Wang¹, Hao Nan Zhang¹, Feng Zhou¹,
and Zi Yao Cheng¹

¹College of Information Engineering
Yancheng Optical Fiber Sensing and Application Engineering Technology Research Center,
Yancheng Institute of Technology, Jiangsu Yancheng 224051, China
949650915@qq.com, kongweibin@ycit.cn, wanglei0324@ycit.edu.cn,
zhanghn0628@163.com, zfcit@163.com, chengziyao041017@163.com

²School of Information Science and Engineering
Southeast University, Jiangsu Nanjing 211189s, China
2106815946@qq.com

Abstract – In this study, a multi-strategy improved gold rush optimizer (MIGRO) is proposed for the design of multilayer broadband microwave absorbers (for normal incidence). The purpose of this optimization process is to minimize the maximum reflection coefficient of the absorber by selecting appropriate material layers from existing literature databases within the desired frequency range. To enhance the performance of a gold rush optimizer (GRO), three improvement strategies are proposed. This paper demonstrates the effectiveness of the improved strategy and the superior reflection coefficient of the MIGRO compared to other heuristic algorithms used for the design of microwave absorbers through two different simulation examples.

Index Terms – Absorbing material, gold rush optimizer, multilayer microwave absorber, reflection coefficient.

I. INTRODUCTION

Microwave absorbing materials are widely applied in fields such as aerospace, construction, and healthcare [1–4]. These materials interact with electromagnetic waves through various mechanisms, including reflection, absorption, transmission, and secondary reflection. By converting electromagnetic energy into thermal energy or other forms of energy, these materials attenuate and absorb electromagnetic waves, thereby reducing their reflection and transmission [5]. With the increasingly complex electromagnetic environment, there is a growing demand for lightweight, high-performance microwave absorbing materials. However, absorbers composed of a single absorbing material have limitations, including narrow absorption bandwidth, lower absorption efficiency, and larger size and weight. In

contrast, multilayer structured absorbing materials offer design flexibility and the ability to compensate for these material defects [6].

In the case of normal incidence, the reflection coefficient of multilayer microwave absorbers depends on various factors such as the frequency of the electromagnetic waves, the electromagnetic parameters, and thickness of each layer of materials. Determining the type of material and adjusting its thickness to reduce the reflection coefficient within the desired frequency range can be considered as an optimization challenge.

Michielssen et al. proposed a physical model for multilayer microwave absorber structures. They provided a set of predefined materials with frequency-dependent electrical permittivity and magnetic permeability, and utilized a genetic algorithm (GA) to determine the optimal material selection and thickness for each layer [7]. Subsequently, various heuristic algorithms have been introduced and successfully applied in designing multilayer microwave absorbers, such as particle swarm optimization (PSO) and its derivatives [8, 9], differential evolution (DE) [10, 11], central force optimization (CFO) [12], a hybrid algorithm of binary lightning search algorithm and simulated annealing (BLSA-SA) [13], and bald eagle search optimization algorithm (BESOA) [14]. A comparative analysis of particle swarm optimization (PSO), bat algorithm (BAT), and cuckoo search algorithm (CSA) was conducted in [15]. With the emergence of new heuristic algorithms, there is still room for further optimization of multilayer microwave absorbers.

In this study, a multi-strategy improved gold rush optimizer (MIGRO) which determines the optimal layer sequence and corresponding thicknesses for the

multilayer microwave absorbers design is proposed. To enhance the convergence speed and global search capability of MIGRO, three improvement strategies were introduced, including quasi-reverse learning, sigmoid convergence weight, and golden sine algorithm. Through two design examples, it was demonstrated that, compared to other heuristic algorithms, MIGRO generated superior reflection coefficients when designing multilayer microwave absorbers.

II. PHYSICAL MODEL OF MULTILAYER ABSORBER

The physical model of a multilayer microwave absorber is shown in Fig. 1, where a uniform plane wave is incident normally on the surface of the absorber. The absorber consists of N planar layers and is supported by a perfect electric conductor (PEC). Each layer in the absorber varies in thickness and possesses magnetic/electrical properties that are dependent on frequency. The thickness of each layer is represented by d_i , while the dielectric constant and magnetic permeability are denoted as ϵ_i and μ_i , respectively. By applying the equivalent transmission line theory of electromagnetic waves, the structure can be represented as a circuit model consisting of cascaded N segment uniform transmission lines [16], as shown in Fig. 2.

The electromagnetic wave absorption performance of multilayer absorbers is evaluated by calculating the return loss value, expressed as equation (1), and used as

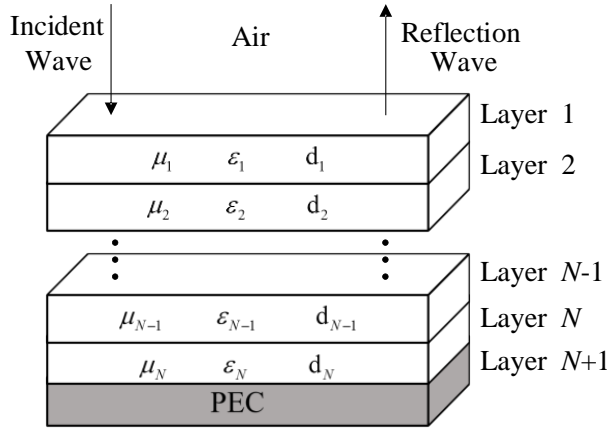


Fig. 1. Physical model of multilayer microwave absorber.

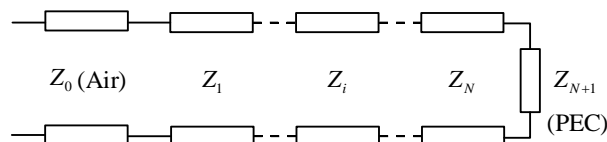


Fig. 2. Equivalent circuit of multilayer microwave absorber.

the objective function for optimization:

$$F_{obj} = 20 \log_{10}(\max |R|). \quad (1)$$

The reflection coefficient at the interface between free space and the medium is denoted as R , and can be formulated as:

$$R = \frac{Z_1 - \eta_0}{Z_1 + \eta_0}, \quad (2)$$

where η_0 is the intrinsic impedance of free space. The total impedance of the absorber is denoted as Z_1 . In the case of normal incidence, the input impedance Z_i of the i -th layer is described as follows:

$$Z_i = \eta_i \frac{Z_{i+1} + j\eta_i \tan(\beta_i d_i)}{\eta_i + jZ_{i+1} \tan(\beta_i d_i)}, i < N. \quad (3)$$

The input impedance of the N -th layer can be considered as the input impedance of the transmission line with a terminal short circuit, which is expressed as follows:

$$Z_i = j\eta_i \tan(\beta_i d_i), i = N, \quad (4)$$

where β_i , d_i , and η_i are the phase constant, thickness, and wave impedance of the i -th layer, respectively. η_i and β_i are defined as follows:

$$\eta_i = \sqrt{\frac{\mu_i}{\epsilon_i}}, \quad (5)$$

$$\beta_i = \frac{2\pi f}{c} \sqrt{\mu_{r,i} \epsilon_{r,i}}, \quad (6)$$

where μ_i and ϵ_i are the magnetic permeability and dielectric constant of the material, $\mu_{r,i}$ and $\epsilon_{r,i}$ are the relative magnetic permeability and relative dielectric constant of the material, f is the frequency, and c is the speed of light.

III. GOLD RUSH OPTIMIZER

A. Basic gold rush optimizer

A gold rush optimizer (GRO) is a metaheuristic algorithm based on population that incorporates three fundamental principles of gold exploration: migration, panning, and collaboration [17]. It has been successfully applied to engineering optimization problems [18, 19].

(1) Migration of prospectors

The mathematical expressions for simulating the process of gold prospectors approaching the gold mine are as follows:

$$D_1 = C_1 \cdot X^{best}(t) - X_i(t), \quad (7)$$

$$X_{new,i}(t+1) = X_i(t) + A_1 \cdot D_1, \quad (8)$$

where X^{best} , X_i , and t represent the values of the optimal solution, the current solution i , and the number of iterations, respectively. $X_{new,i}$ denotes the new position of feasible solutions, and the expressions for A_1 and C_1 are as follows:

$$A_1 = 1 + l_1 \left(k_1 - \frac{1}{2} \right), \quad (9)$$

$$C_1 = 2k_2, \quad (10)$$

where k_1 and k_2 are uniformly distributed random numbers in the range $[0, 1]$. l_1 is the convergence factor, defined as follows:

$$l_1 = 2 + \left(\frac{1-t}{t_{\max}-1} \right) \left(2 - \frac{1}{t_{\max}} \right). \quad (11)$$

(2) Gold mining

In pursuit of the golden dream, gold prospectors continuously adjust their positions to obtain more gold, and the expression of the gold mining process is as follows:

$$D_2 = X_i(t) - X_r(t), \quad (12)$$

$$X_{new,i}(t+1) = X_r(t) + A_2 \cdot D_2, \quad (13)$$

where X_r represents the position of the gold prospector r randomly selected from the feasible solution space, and A_2 is the vector coefficient, as shown in the following equation:

$$A_2 = l_2(2k_1 - 1), \quad (14)$$

where l_2 is defined as follows:

$$l_2 = \left(\frac{t_{\max}-t}{t_{\max}-1} \right)^2 \left(2 - \frac{1}{t_{\max}} \right) + \frac{1}{t_{\max}}. \quad (15)$$

(3) Collaboration

At times, gold prospectors may collaborate with each other to increase the probability of discovering gold, and this collaborative behavior can be represented by the following equation:

$$D_3 = X_{g2}(t) - X_{g1}(t), \quad (16)$$

$$X_{new,i}(t+1) = X_i(t) + k_1 \cdot D_3, \quad (17)$$

where X_{g1} and X_{g2} are two prospectors randomly selected from the expected gold-seeking region, and D_3 is the collaboration vector.

B. Improved gold rush optimizer

A high-quality initial population can improve the solution accuracy and convergence speed of the algorithm. However, the basic GRO employs a random initialization method, which does not guarantee diversity within the initial population. Therefore, the quasi-reverse learning is utilized for the population initialization of GRO. Previous studies have already demonstrated that the utilization of quasi-reverse numbers has been found to be more effective in locating the global optimal solution compared to the use of opposite numbers [20].

Assuming that the value of the i -th gold prospector is represented as X_i , where ub_i is the upper bound of the independent variable X_i and lb_i is the lower bound of the independent variable X_i . The corresponding opposite point X_i^o and quasi-reverse point X_i^{qo} are shown as follows:

$$X_i^o = lb_i + ub_i - X_i, \quad (18)$$

$$X_i^{qo} = \frac{lb_i + ub_i}{2} + \left| X_i^o - \frac{lb_i + ub_i}{2} \right| \cdot rand(0, 1). \quad (19)$$

The GRO employs linear inertia weights, with the value of l_1 decreasing linearly from 2 to 0 as the number of iterations increases. Although this linear inertia weight can partially balance global and local search efforts, the actual search process is highly complex and nonlinear. Consequently, linear weights may diminish the optimization performance of the algorithm.

In this study, MIGRO utilizes the sigmoid function as the nonlinear convergence factor S , replacing the original convergence factor l_1 . The value of S nonlinearly decreases from approximately 2 to nearly 0, as illustrated in Fig. 3, with its corresponding expression defined as follows:

$$S = \frac{2}{\left(1 + \exp\left(\frac{10t}{t_{\max}} - 5 \right) \right)}. \quad (20)$$

The sigmoid function is a nonlinear convergence factor that effectively balances global and local search. It improves the accuracy of population optimization and accelerates optimization speed [21].

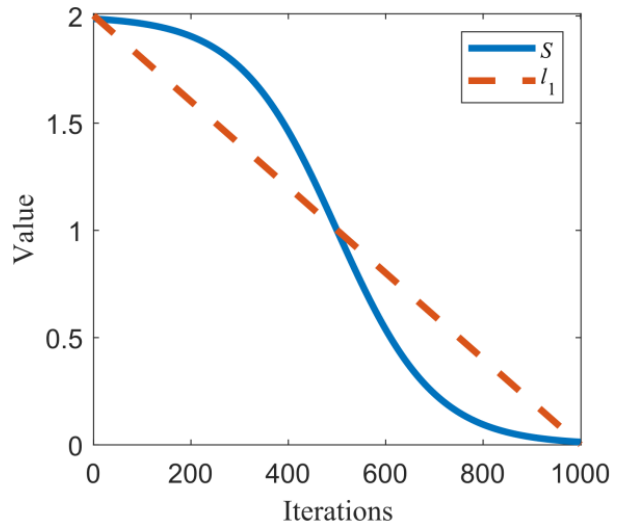


Fig. 3. Graph for values of S during algorithm iteration.

The golden sine algorithm is inspired by the sine function and the golden ratio, where individuals explore the search space based on the golden ratio for approximate optimal solutions. By combining the sine function and the golden ratio, the algorithm can quickly locate the region where the optimal value lies and escape local optima. As a result, the algorithm's performance is improved [22].

Building upon the gold mining and cooperation stages of the GRO, this paper enhances the migration stage of prospectors by incorporating the golden sine algorithm. The position update formula for this process, after integrating the golden sine algorithm, can be

expressed as follows:

$$X_{new,i}(t+1) = X_i(t) \cdot |\sin(R_1)| + R_2 \cdot \sin(R_1) \cdot D^*, \quad (21)$$

$$D^* = d_1 \cdot X^*(t) - d_2 \cdot X_i(t), \quad (22)$$

where R_1 is a random number in the range $[0, 2\pi]$, R_2 is a random number between $[0, \pi]$. d_1 and d_2 are coefficient factors, which can be obtained from the following equation:

$$d_1 = a \cdot \tau + b \cdot (1 - \tau), \quad (23)$$

$$d_2 = a \cdot (1 - \tau) + b \cdot \tau, \quad (24)$$

where a and b are the search interval, which are $-\pi$ and π . τ denotes the golden ratio, which is $(\sqrt{5} - 1)/2$.

The flow chart of MIGRO is shown in Fig. 4.

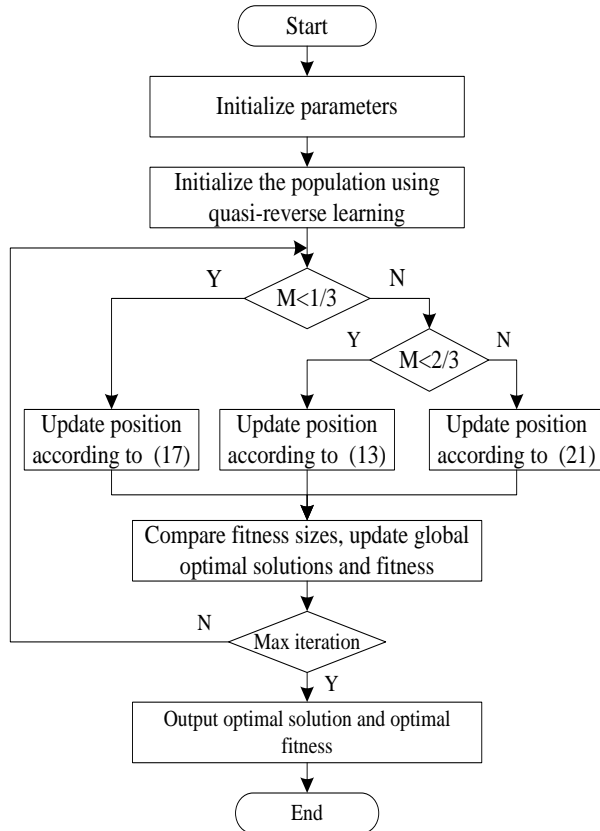


Fig. 4. Flow chart of MIGRO.

IV. SIMULATION EXPERIMENT AND RESULT ANALYSIS

A. Simulation process

In this simulation experiment, the reflection coefficient of the multilayer absorber physical model is determined by the electromagnetic parameters of each layer material, layer thickness, layer arrangement order, and the incident frequency of electromagnetic waves. During the initialization phase, the thickness and material of each layer are randomly assigned, with constraints on the

number of layers, maximum thickness, and bandwidth. As a result, the number of variables is twice the number of layers. The purpose of optimization is to determine the thickness and type of materials for each layer in order to reduce the maximum reflection coefficient.

This database consists of 16 materials, which are categorized into four groups: lossless dielectric materials, lossy magnetic materials, lossy dielectric materials, and relaxation magnetic materials. The relative dielectric constant and magnetic permeability of these materials are summarized in Table 1. These materials are

Table 1: Database of absorbing materials

Lossless dielectric materials ($\mu' = 1, \mu'' = 0$)				
#	ϵ'			
1	10			
2	50			
Lossy magnetic materials ($\epsilon' = 15, \epsilon'' = 0$)				
$\mu = \mu' - j\mu'' \quad \mu' = \frac{\mu'(1\text{GHz})}{f^a} \quad \mu'' = \frac{\mu''(1\text{GHz})}{f^b}$				
#	$\mu'(1\text{GHz})$	a	$\mu''(1\text{GHz})$	b
3	5	0.974	10	0.961
4	3	1.000	15	0.957
5	7	1.000	12	1.000
Lossy dielectric materials ($\mu' = 1, \mu'' = 0$)				
$\epsilon = \epsilon' - j\epsilon'' \quad \epsilon' = \frac{\epsilon'(1\text{GHz})}{f^a} \quad \epsilon'' = \frac{\epsilon''(1\text{GHz})}{f^b}$				
#	$\epsilon'(1\text{GHz})$	a	$\epsilon''(1\text{GHz})$	b
6	5	0.861	8	0.569
7	8	0.778	10	0.682
8	10	0.778	16	0.861
Relaxation-type magnetic materials ($\epsilon' = 15, \epsilon'' = 0$)				
$\mu = \mu' - j\mu'' \quad \mu'(f) = \frac{\mu_m f_m^2}{f^2 + f_m^2} \quad \mu''(f) = \frac{\mu_m f_m f}{f^2 + f_m^2}$				
f and f_m in GHz				
#	μ_m	f_m		
9	35	0.8		
10	35	0.5		
11	30	1.0		
12	18	0.5		
13	20	1.5		
14	30	2.5		
15	30	2.0		
16	25	3.5		

pre-defined and also used in [7–15]. The selection of these materials is made in order to maintain consistency in the comparison.

The mathematical modeling and optimization process of multilayer microwave absorbers was implemented using MATLAB R2022A software. CST Studio Suite is a powerful 3D electromagnetic field simulation software. The optimal material types and layer thickness obtained through numerical calculations will be imported into CST for electromagnetic simulation, ensuring the accuracy of the optimization results.

B. Results and analysis

This section introduces two design examples to demonstrate the advantages of MIGRO in designing multilayer microwave absorbers. The results obtained from the MIGRO and the basic GRO are compared with those of other heuristic algorithms published in the literature.

(1) First example: 5-layer absorber

This 5-layer absorber is designed to operate within the frequency range 2-8 GHz, with a frequency step of 0.1 GHz and a total thickness constraint of 5 mm. For this experiment, the population size for both MIGRO and GRO is set to 50, with a maximum iteration limit of 1000 iterations. Each algorithm is independently run 20 times. The optimization results obtained from the BESOA [14], BLSA-SA [13], and CFO [12] methods are compared with the results of the present experiment, as shown in Table 2.

MIGRO achieves the best maximum reflection coefficient within the frequency range 2-8 GHz, while also maintaining the lowest average reflection coefficient. The corresponding reflection coefficients are shown in Fig. 5, with MIGRO reaching a peak of -33.2748 dB at 2.4 GHz. Figure 6 displays the convergence curves of MIGRO and GRO.

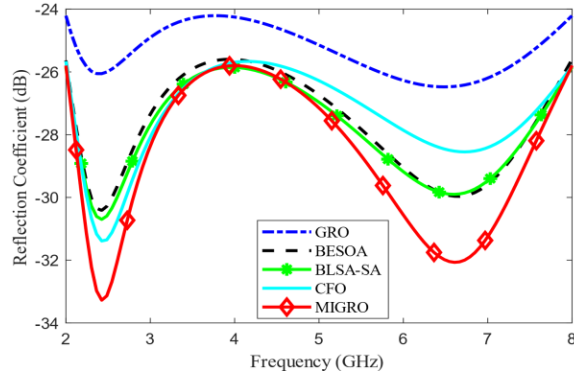


Fig. 5. Comparison of reflection coefficients for 5-layer designs in the 2-8 GHz.

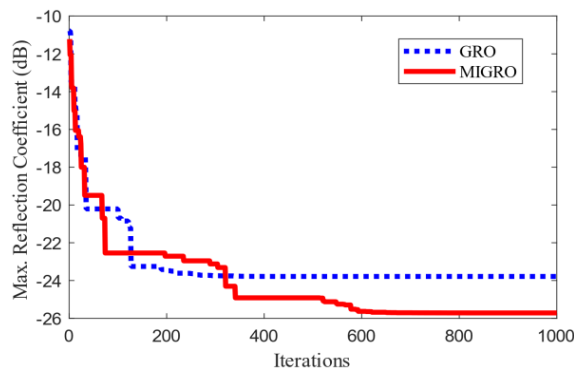


Fig. 6. Comparison of convergence curves for 5-layer designs over 1000 iterations.

MIGRO demonstrates higher convergence accuracy in the later stages than GRO, indicating that the improved strategies of the algorithm effectively prevent MIGRO from getting trapped in local optima.

Table 2: The best optimization results of 5-layer microwave absorber

Algorithm	MIGRO		GRO		BESOA [14]		BLSA-SA [13]		CFO [12]	
Layers	Type and Thickness									
1	16	0.3771	16	0.4097	16	0.41701	16	0.3682	16	0.377
2	6	0.8308	6	1.0306	6	1.10903	6	1.9580	6	1.572
3	6	1.3524	6	1.2394	6	1.78825	6	1.1016	6	0.991
4	6	1.0659	11	0.8852	3	0.21456	14	0.4834	6	0.377
5	14	1.3550	13	1.0732	15	1.27113	15	0.9424	15	1.425
Total thickness (mm)	4.9812		4.6381		4.79998		4.8536		4.744	
Max. reflection coefficient (dB)	-25.8852		-24.2055		-25.765		-25.8528		-25.698	
Avg. reflection coefficient (dB)	-28.7024		-25.3212		-27.7014		-27.8752		-27.4246	

(2) Second example: 7-layer absorber

In this instance, the 7-layer absorber was optimized with a maximum total thickness constraint of 10 mm. To investigate the optimization results across a broader frequency range, the absorption bandwidth was extended to 0.1-20 GHz. The remaining experimental parameters remain consistent with the initial example.

The design results of MIGRO were compared with the results of BLSA-SA [14], CAS [15], and DE [11]. As shown in Table 3, the maximum reflection coefficients of MIGRO, GRO, [14], [15], and [11] are -18.3183 , -18.0175 , -18.0406 , -18.0879 , and -17.9 dB, respectively. MIGRO exhibits the lowest maximum reflection coefficient. Additionally, MIGRO also has the lowest average reflection coefficient of -19.6811 dB. In Fig. 7, the reflection coefficients in the frequency range 0.1-20 GHz are calculated using five intelligent algorithms. From Fig. 8, it can be seen that, compared to GRO, MIGRO exhibits higher convergence accuracy in iterations.

C. Verify simulation results with CST

Computer Simulation Technology (CST) Microwave Studio Suite (MWS) is a commonly utilized electromagnetic simulation software that has been employed to validate the efficacy of numerous multilayer microwave absorbers designs [23, 24]. For this research, all simulations were carried out using the Finite Element Method (FEM) and Frequency Domain Solver (FDS) modules within CST.

Materials 3 to 16 from Table 1 were imported into the CST material library. To incorporate the material property parameters provided externally, CST Studio utilized fitting techniques internally to store the provided

data. The fitting error between the original provided data and the fitted data will result in deviations between

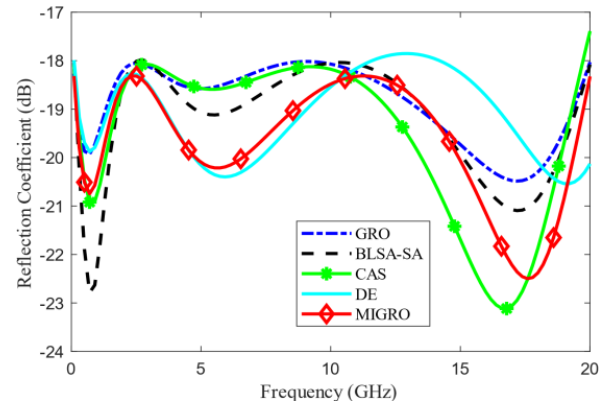


Fig. 7. Comparison of reflection coefficients for 7-layer designs in the 0.1-20 GHz range.

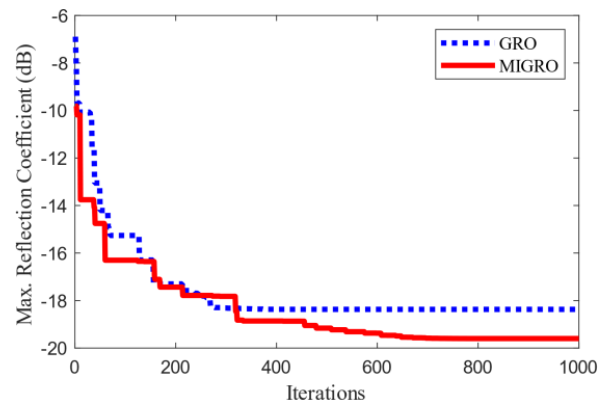


Fig. 8. Comparison of convergence curves for 7-layer designs over 1000 iterations.

Table 3: The best optimization results of 7-layer microwave absorber

Algorithm	MIGRO		GRO		BLSA-SA [14]		CAS [15]		DE [11]	
Layers	Type and Thickness									
1	16	0.2131	16	0.2114	16	0.2080	16	0.2107	14	0.2064
2	6	2.0127	6	1.7644	6	1.7490	6	1.1066	6	1.8762
3	14	0.5994	14	0.5457	16	0.0850	6	0.7916	16	0.5391
4	6	0.9139	3	1.9669	6	0.0820	14	0.5482	6	0.9499
5	5	1.6448	6	2.2745	14	0.4922	5	1.3785	5	1.9596
6	4	0.6706	4	1.6528	5	1.5020	6	0.5570	4	0.7817
7	5	0.9627	6	0.2784	4	1.6602	4	1.7450	5	0.4864
Total thickness (mm)	7.0172		8.6941		5.7784		6.3376		6.7993	
Max. reflection coefficient (dB)	-18.3183		-18.0175		-18.0406		-18.0879		-17.9	
Avg. reflection coefficient (dB)	-19.6811		-18.8682		-19.2074		-19.5157		-19.1169	

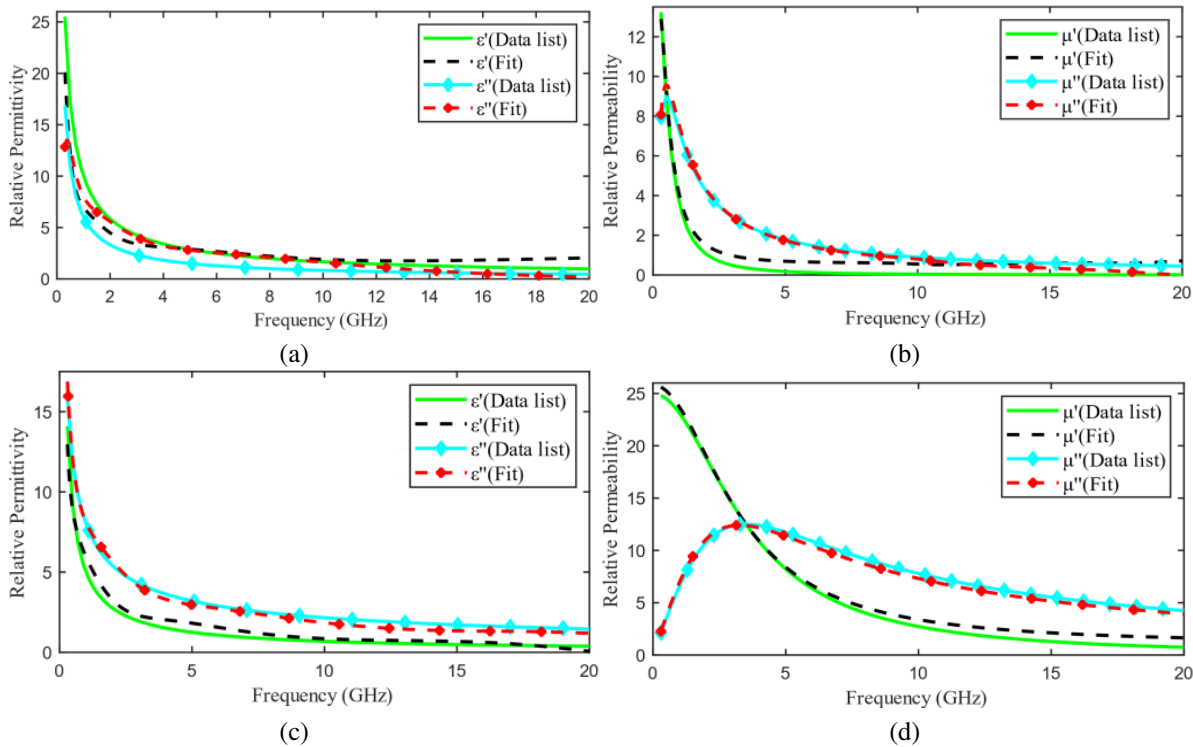


Fig. 9. Comparison of supplied and fitted material dispersion curves in CST: (a) Material 8, (b) Material 12, (c) Material 6, and (d) Material 16.

the simulated results in CST and the calculated results [25]. Among all these materials, Materials 8 and 12 exhibit relatively large fitting errors. For comparison, Figs. 9 (a)-(d) illustrate the fitting data for Materials 8, 12, 6, and 16, respectively.

Using the 5-layer optimal design as an example, a multilayer microwave absorber model is constructed in CST where the material type and thickness of each layer align with the MIGRO data presented in Table 2. The absorber structure is simulated as an infinite periodic repetition (unit cell) along the x and y axes. Two Floquet

ports are defined at both the maximum (Z_{max}) and minimum (Z_{min}) of the $z - axis$, with a plane wave incidence angle set to 0 degrees and a frequency range 2-8 GHz, feasibly generating the plane wave model, as illustrated in Fig. 10.

In the CST simulation results, the reflection coefficient curves for the 5-layer and 7-layer optimized designs are shown in Figs. 11 (a)-(b). The numerical calculation results and the electromagnetic simulation results exhibit no significant discrepancies, thereby

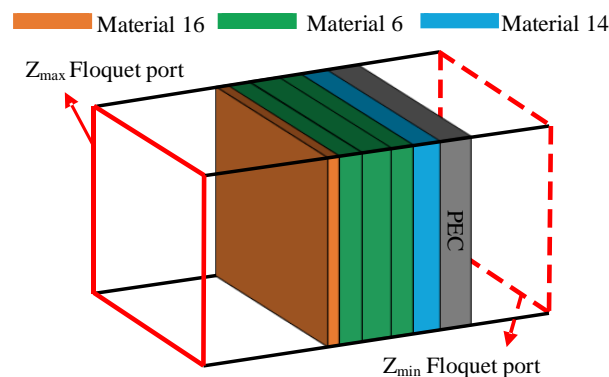


Fig. 10. Model of the 5-layer absorber and the two Floquet ports used to excite the plane waves.

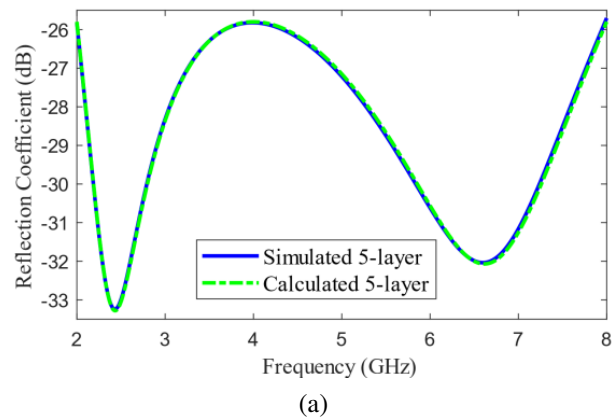


Fig. 11. Continued

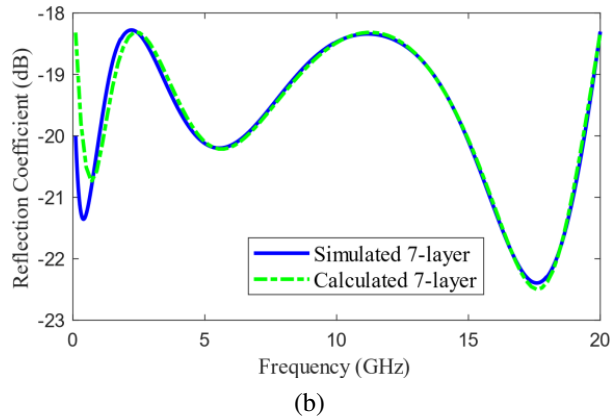


Fig. 11. Comparison of reflectance coefficients calculated by MIGRO and simulated by CST: (a) 5-layer at 2-8 GHz and (b) 7-layer at 0.1-20 GHz.

validating the accuracy of the mathematical modeling and algorithm optimization process for the multilayer microwave absorber.

V. CONCLUSION

This paper presents MIGRO that combines three strategies for the optimization design of the multilayer microwave absorbers under normal incident conditions. This method can be used to obtain a set of coatings with the minimum reflection coefficients within a specific frequency and thickness range. Two multilayer absorbers were designed for 2-8 GHz, 5-layer, and 0.1-20 GHz, 7-layer scenarios, and their design results were compared with those of other algorithms published in the literature. In both cases, MIGRO exhibits lower maximum and average reflection coefficients compared to other algorithms. Therefore, the effectiveness of the improvement strategy has been validated, indicating that MIGRO have stronger optimization capabilities.

ACKNOWLEDGMENT

This work was supported by Postgraduate Research & Practice Innovation Program of Jiangsu Province (Grant No. SJCX23-1871, No. SJCX23-XY069 and No. SJCX23-XY071), College Students Innovation and Entrepreneurship Training Program (Grant No. 2023591 and No. 2023576), Yancheng Institute of Technology Teaching Reform Research Project under Grant No. YKT2022A028.

REFERENCES

- [1] R. Panwar, S. Puthucheri, D. Singh, and V. Agarwala, "Design of ferrite-graphene-based thin broadband radar wave absorber for stealth application," *IEEE Transactions on Magnetics*, vol. 51, no. 11, pp. 1-4, Nov. 2015.
- [2] A. Delfini, M. Albano, A. Vricella, F. Santoni, G. Rubini, R. Pastore, and M. Marchetti, "Advanced radar absorbing ceramic-based materials for multifunctional applications in space environment," *Materials*, vol. 11, no. 9, p. 1730, Sep. 2018.
- [3] S. Xie, Z. Ji, L. Zhu, J. Zhang, Y. Cao, J. Chen, R. Liu, and J. Wang, "Recent progress in electromagnetic wave absorption building materials," *Journal of Building Engineering*, vol. 27, p. 100963, Jan. 2022.
- [4] S. Ren, H. Yu, L. Wang, Z. Huang, T. Lin, Y. Huang, J. Yang, Y. Hong, and J. Liu, "State of the art and prospects in metal-organic framework-derived microwave absorption materials," *Nano-Micro Letters*, vol. 14, no. 1, p. 68, Feb. 2022.
- [5] H. Pang, Y. Duan, L. Huang, L. Song, J. Liu, T. Zhang, X. Yang, J. Liu, X. Ma, J. Di, and X. Liu, "Research advances in composition, structure and mechanisms of microwave absorbing materials," *Composites Part B: Engineering*, vol. 224, p. 109173, Nov. 2021.
- [6] R. Panwar and J. R. Lee, "Recent advances in thin and broadband layered microwave absorbing and shielding structures for commercial and defense applications," *Functional Composites and Structures*, vol. 1, no. 3, p. 032022, July 2019.
- [7] E. Michielssen, J. M. Sajer, S. Ranjithan, and R. Mittra, "Design of lightweight, broad-band microwave absorbers using genetic algorithms," *IEEE Transactions on Microwave Theory and Techniques*, vol. 41, no. 6, pp. 1024-1032, June/July 1993.
- [8] S. Chamaani, S. A. Mirtaheri, and M. A. Shooredeli, "Design of very thin wide band absorbers using modified local best particle swarm optimization," *AEU-International Journal of Electronics and Communications*, vol. 62, no. 7, pp. 549-556, Aug. 2008.
- [9] S. Roy, S. D. Roy, J. Tewary, A. Mahanti, and G. Mahanti, "Particle swarm optimization for optimal design of broadband multilayer microwave absorber for wide angle of incidence," *Progress in Electromagnetics Research B*, vol. 62, pp. 121-135, Feb. 2015.
- [10] S. K. Goudos, "Design of microwave broadband absorbers using a self-adaptive differential evolution algorithm," *International Journal of RF and Microwave Computer-Aided Engineering*, vol. 19, no. 3, pp. 364-372, Apr. 2009.
- [11] N. I. Dib, M. Asi, and A. Sabbah, "On the optimal design of multilayer microwave absorbers," *Progress in Electromagnetics Research C*, vol. 13, pp. 171-185, 2010.

- [12] M. Asi and N. I. Dib, "Design of multilayer microwave broadband absorbers using central force optimization," *Progress in Electromagnetics Research B*, vol. 26, pp. 101-113, 2010.
- [13] Y. Lu and Y. Zhou, "Design of multilayer microwave absorbers using hybrid binary lightning search algorithm and simulated annealing," *Progress in Electromagnetics Research B*, vol. 78, pp. 75-90, 2017.
- [14] S. Kankılıç and E. Karpat, "Optimization of multilayer absorbers using the bald eagle optimization algorithm," *Applied Sciences*, vol. 13, no. 18, p. 10301, Sep. 2023.
- [15] S. Roy, A. Mahanti, S. D. Roy and G. K. Mahanti, "Comparison of evolutionary algorithms for optimal design of broadband multilayer microwave absorber for normal and oblique incidence," *Applied Computational Electromagnetics Society (ACES) Journal*, vol. 31, no. 1, pp. 79-84, Jan. 2016.
- [16] T. Wang, G. Chen, J. H. Zhu, H. Gong, L. M. Zhang, and H. J. Wu, "Deep understanding of impedance matching and quarter wavelength theory in electromagnetic wave absorption," *Journal of Colloid and Interface Science*, vol. 595, pp. 1-5, Aug. 2021.
- [17] K. Zolf, "Gold rush optimizer: A new population-based metaheuristic algorithm," *Operations Research and Decisions*, vol. 33, no. 1, pp. 113-150, 2023.
- [18] M. Saglam, Y. Bektas, and O. A. Karaman, "Dandelion optimizer and gold rush optimizer algorithm-based optimization of multilevel inverters," *Arabian Journal for Science and Engineering*, vol. 49, pp. 7029-7052, Jan. 2024.
- [19] H. Abdelfattah, M Esmail, S. A. kotb, M. M. Mahmoud, H. S. Hussein, D. E. M. Wapet, A. I. Omar, and A. M. Ewais, "Optimal controller design for reactor core power stabilization in a pressurized water reactor: Applications of gold rush algorithm," *Plos One*, vol. 19, no. 1, p. e0287772, Jan. 2024.
- [20] Z. Wang, L. Huang, S. Yang, D. Li, D. He, and S. Chan, "A quasi-oppositional learning of updating quantum state and Q-learning based on the dung beetle algorithm for global optimization," *Alexandria Engineering Journal*, vol. 81, pp. 468-488, Oct. 2023.
- [21] W. Liu, Z. Wang, Y. Yuan, N. Zeng, K. Hone, and X. Liu, "A novel sigmoid-function-based adaptive weighted particle swarm optimizer," *IEEE Transactions on Cybernetics*, vol. 51, no. 2, pp. 1085-1093, July 2019.
- [22] Q. Liu, N. Li, H. Jia, Q. Qi, L. Abualigah, and Y. Liu, "A hybrid arithmetic optimization and golden sine algorithm for solving industrial engineering design problems," *Mathematics*, vol. 10, no. 9, p. 1567, May 2022.
- [23] E. Yigit and H. Duysak, "Determination of optimal layer sequence and thickness for broadband multilayer absorber design using double-stage artificial bee colony algorithm," *IEEE Transactions on Microwave Theory and Techniques*, vol. 67, no. 8, pp. 3306-3317, Aug. 2019.
- [24] H. Yao, J. Yang, H. Li, J. Xu, and K. Bi, "Optimal design of multilayer radar absorbing materials: A simulation-optimization approach," *Advanced Composites and Hybrid Materials*, vol. 6, no. 1, p. 43, Jan. 2023.
- [25] P. Warhekar, A. Bhattacharya, and S. Neogi, "Designing thinner broadband multilayer radar absorbing material through novel formulation of cost function," *IEEE Access*, vol. 11, pp. 91016-91027, Oct. 2023.



Yi Ming Zong received the B.S. degree in electronic information engineering from Yancheng Institute of Technology in 2022. He is currently pursuing the M.Eng. degree in electronic information at Yancheng Institute of Technology. His main research interests focus on computational electromagnetics and artificial intelligence.



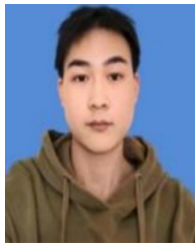
Wei Bin Kong received the B.S. degree in mathematics from Qufu Normal University, China, 2007, the M.S. degree in mathematics from Southeast University, Nanjing, China, in 2010, and the Ph.D. degree in radio engineering from Southeast University, Nanjing, China, in 2015. Since 2020, he has been an associate professor with the College of Information Engineering, Yancheng Institute of Technology, Yancheng. His current research interests include computational electromagnetism, artificial intelligence, and wireless communication.



Jia Pan Li received the B.S. degree in college of information and communication engineering from Harbin Engineering University. He is currently working toward the master's degree in electronic and information engineering at Southeast University. His current research interests include signal processing and optimum algorithms.



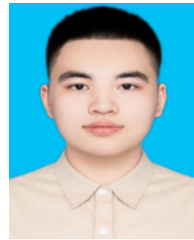
Lei Wang received the B.S. degree in integrated circuit design and integrated systems and the Ph.D. degree in information and communication engineering from Nantong University, Nantong, Jiangsu, China, in 2017 and 2023, respectively. Since 2023, he has been a Lecturer with the College of Information Engineering, Yancheng Institute of Technology, Yancheng. His current research interests include artificial intelligence and antenna, millimeter-wave antennas and arrays, and characteristic mode analysis.



Hao Nan Zhang received the B.S. degree from the Southeast University Chengxian College, Nanjing, China, in 2021, and he is currently pursuing the M.Eng. degree at Yancheng Institute of Technology. His current research interests include computational electromagnetics and wireless communications.



Feng Zhou received the B.S. degrees and M.S. degrees from Southeast University, Nanjing, China, in 2004 and 2012, respectively. Since 2023, he is a professor with the College of Information Engineering, Yancheng Institute of Technology, Yancheng, China. His research interests include cooperative communication, satellite communication, cognitive radio, physical layer security, and UAV communication.



Zi Yao Cheng is currently pursuing the bachelor's degree in optoelectronic information engineering with Yancheng Institute of Technology. During the bachelor's degree, he actively participated in multiple research projects on object detection and made outstanding contributions to optimizing object detection models. His research interests include computer vision and intelligent algorithms.